Biochemical and Biophysical Research Communications 482 (2017) 1194–1200

Contents lists available at ScienceDirect

Biochemical and Biophysical Research Communications

journal homepage: www.elsevier.com/locate/ybbrc

# Development of a novel catalytic amyloid displaying a metal-dependent ATPase-like activity

Octavio Monasterio, Esteban Nova, Rodrigo Diaz-Espinoza*

*Laboratorio de Biología Estructural y Molecular, Departamento de Biología, Facultad de Ciencias, Universidad de Chile, Santiago, Chile*

ARTICLE INFO

*Article history:*
Received 19 November 2016
Accepted 2 December 2016
Available online 3 December 2016

*Keywords:*
Amyloid
Peptide
Catalysis
Hydrolysis
ATP
Manganese

ABSTRACT

Amyloids are protein aggregates of highly regular structure that are involved in diverse pathologies such as Alzheimer's and Parkinson's disease. Recent evidence has shown that under certain conditions, small peptides can self-assemble into amyloids that exhibit catalytic reactivity towards certain compounds. Here we report a novel peptide with a sequence derived from the active site of RNA polymerase that displays hydrolytic activity towards ATP. The catalytic reaction proceeds in the presence of the divalent metal manganese and the products are ADP and AMP. The kinetic data shows a substrate-dependent saturation of the activity with a maximum rate achieved at around 1 mM ATP. At higher ATP concentrations, we also observed substrate inhibition of the activity. The self-assembly of the peptide into amyloids is strictly metal-dependent and required for the catalysis. Our results show that aspartate-containing amyloids can also be catalysts under conditions that include interactions with metals. Moreover, we show for the first time an amyloid that exerts reactivity towards a biologically essential molecule.



## 1. Introduction

Amyloids are highly ordered protein aggregates that have been classically associated to relevant pathologies such as Alzheimer's, Parkinson's and Prion diseases among others [1]. Their overall structural architecture is characterized by a cross-beta fold that grows along a central axis to form large filaments [2,3]. The involvement of amyloids in several pathologies has labeled them as toxic particles, although no universal mechanism for toxicity has yet been established [4]. In recent years however, increasing evidence of non-toxic functional amyloids has been reported [5]. Their unique mechanical and structural features can be exploited by nature to carry novel functions such as biofilm formation, transcriptional regulation, hormone storage, etc. [6–8]. These works have also led to propose amyloids as novel bio-nanomaterials that can have diverse biotechnological applications [9].

The diverse properties of amyloids have recently been expanded with the discovery of catalytic reactivity emerging from small self-assembled peptides [10,11]. These rationally designed catalytic amyloids exhibited potent esterase activity towards the model compound p-nitrophenylacetate when histidine residues were alternated with hydrophobic groups in the peptide sequences [10]. The solvent-exposed histidines were shown to coordinate zinc ions ($Zn^{+2}$) to form catalytically active amyloid-metal complexes that showed enzymatic-like features from the kinetic data. In a more recent report, different histidine-containing peptides displaying similar esterase activity emerged from a random peptide library using a central amyloid-prone motif [11]. These findings can have important implications that include not only a putative involvement of amyloid catalytic reactivity in cellular toxicity but also a plausible role in molecular evolution. In fact, amyloids have been proposed as potentially relevant prebiotic entities due to their unique physical properties such as spontaneous self-assembly of their peptide constituents and high stability against environmental changes including temperature and pH, among others [12]. The discovery of catalytic reactivity emerging from amyloids may imply that small prebiotic peptides can in principle harbor novel functionalities. Interestingly, mixtures of several amino acids considered prebiotic have recently been shown to yield peptides that spontaneously self-assembled into amyloid structures, providing a proof of principle to this idea [13].

In the present study, we report the design and development of a novel catalytic amyloid that displayed hydrolytic activity towards

*Abbreviations:* Th-T, Thioflavin-T; $Mg^{+2}$, magnesium ion; $Mn^{+2}$, manganese ion; ATP, adenosine triphosphate.

* Corresponding author. Las Palmeras 3425, Santiago, CP7800003, Chile.
*E-mail address:* rodrigo.diaz.e@u.uchile.cl (R. Diaz-Espinoza).

http://dx.doi.org/10.1016/j.bbrc.2016.12.011
0006-291X/

ATP in a metal-dependent manner. We initially studied the assembly of the peptide into amyloids in presence of divalent metals. The catalytic reactivity of the peptide towards the nucleotide was characterized under different experimental conditions that were then correlated with the formation of the amyloid. Overall, our results show for the first time a catalytic amyloid with reactive acidic groups that through interaction with manganese can hydrolyze a physiologically important molecule.

## 2. Materials and methods

### 2.1. Chemicals

Peptides were purchased from Genscript (NJ, USA) at the highest available purity (>98%) with their both end terminals capped (N-terminal acetylated and C-terminal amidated). All other chemical reagents were purchased from Sigma-Aldrich (St. Louis, MO, USA).

### 2.2. Peptide stock and sample preparation

Lyophilized peptides were dissolved in 10 mM sodium hydroxide (NaOH) followed by sonication in cold water to make a 4 mM stock solution. The reactions were prepared by diluting the stock solution to the required peptide concentrations in 50 mM Tris-HCl pH 8.0. Divalent metals ($MgCl_2$ or $MnCl_2$) were added at 10 mM final concentration when specified. For peptide control reactions, 10 mM NaOH was added instead of peptide stock in an equivalent volume. Kinetic experiments were run in the same conditions but with presence of adenosine triphosphate (ATP) at the specified concentrations. The residual metal-dependent hydrolysis in absence of peptides was subtracted from the experimental samples to determine hydrolytic activities. All reactions rates are expressed as the sum of the products ADP (adenosine diphosphate) plus AMP (adenosine monophosphate). Time-course aggregation experiments were performed using the aforementioned conditions (with or without ATP) plus 25 μM of the fluorescent amyloid-specific Thioflavin-T probe (Th-T) that significantly increases its emission fluorescence upon binding to amyloids [14]. Catalysis and aggregation reactions were run at 37C with continuous agitation.

### 2.3. Fluorescence spectroscopy

Time-course aggregations were run in black 96-well plates (4titude, UK) sealed with optically clear films (Bio-Rad, UK) using continuous bottom reading mode at 37 °C in a Tecan Infinite 200 PRO system with automatic measurement every 15 min for specified times. Excitation and emission fluorescence were set at 435 nm and 485 nm respectively according to literature [14]. Emission spectra were recorded from 460 nm to 600 nm with an excitation of 435 nm using optimized gain.

### 2.4. Transmission electron microscopy (TEM)

Samples with aggregated peptides were adsorbed to UV-treated Formvar carbon-coated grids (Electron Microscopy Sciences) for 2 min followed by washed with milli-Q water. Negative staining was performed using 2% uranyl acetate (2 min). Pictures were taken with a 120 kV PHILIPS FEI Tecnai-12 BioTwin electron microscope using a Gatan-Orius®1000 dual-scan CCD camera.

### 2.5. High performance liquid chromatography (HPLC) analyses

Reaction samples were centrifuged at 14.000*g* and the supernatant was analyzed by ion-pair chromatography. Samples were loaded onto a C-18 column and then run on HPLC system (Beckman System Gold) using 50 mM $K_2HPO_4$, 20 mM glacial acetic acid, 8% (V/V) acetonitrile and 4 mM tetrabutylammonium phosphate monobasic for the mobile phase. Stock solutions of the nucleotide standards ATP, ADP and AMP were used to determine retention times. All samples were analyzed by absorbance with the HPLC detector set at 260 nm.

### 2.6. Computational analysis of amyloidogenic propensity

Protein sequences were analyzed with the ZipperDB algorithm to search for amyloid-prone regions [15,16]. The algorithm default parameters provide amyloidogenic energies (Rosetta energy) in 6-mer windows so longer sequences are analyzed by sequentially shifting the window. Segments with Rosetta energies lower than −23 kcal/mol are considered amyloidogenic.

## 3. Results

### 3.1. Peptide design and aggregation

The development of catalytic amyloids has been previously accomplished by designing peptide sequences directly extracted from the active site of enzymes with histidine residues that can coordinate divalent metals such as $Zn^{+2}$ [10]. We therefore asked whether a similar approach could be used to design catalytic amyloids with active acidic residues. A known group of enzymes that use acidic residues for metal coordination in their active sites is the superfamily of Nucleotidyltransferases (NTases) [17,18]. These enzymes are reactive towards nucleotides and perform their activities by coordinating magnesium ($Mg^{+2}$) and/or manganese ($Mn^{+2}$) ions to aspartate/glutamate residues. By looking at the sequences of different NTases we found that the active site of RNA polymerases contains three conserved catalytic aspartates involved in metal coordination in a highly conserved sequence (NADFDGD). We analyzed the amyloid propensity of this sequence by using the ZipperDB algorithm and found that in some organisms such as *Thermus acquaticus* the aspartates are followed by a highly amyloidogenic fragment (sequence QMAVHV, Table 1). The catalytic region exhibited low amyloid propensity probably due to strong electrostatic repulsion from the aspartate groups. We therefore synthesized a peptide containing both the catalytic fragment and its adjacent amyloidogenic region (NADFDGDQMAVHV) and tested its aggregation.

Fig. 1A shows that over a 48-hr incubation of the peptide at 37C the averaged maximum emission fluorescence of the amyloid-specific dye Th-T did not increase unless $Mg^{+2}$ or $Mn^{+2}$ were added at millimolar concentrations. Both metals induced a strong and similar switch to the amyloid state that increased the baseline Th-T signal around 10 times. The Th-T spectra of the $Mn^{+2}$-induced amyloids shows the typical shape observed for amyloids with a

**Table 1**
Rosetta energies for peptide NADFDGDQMAVHV.

| Peptide Sequence | Segment Analyzed[a] | Rosetta Energy (kcal/mol) |
|---|---|---|
| NADFDGDQMAVHV | NADFDG | −15.9 |
| | ADFDGD | −14.5 |
| | DFDGDQ | −13.1 |
| | FDGDQM | −16.6 |
| | DGDQMA | −17.5 |
| | GDQMAV | −22.2 |
| | DQMAVH | −23.0 |
| | QMAVHV[a] | −27.0 |

[a] The amyloidogenic region QMAVHV is underlined.

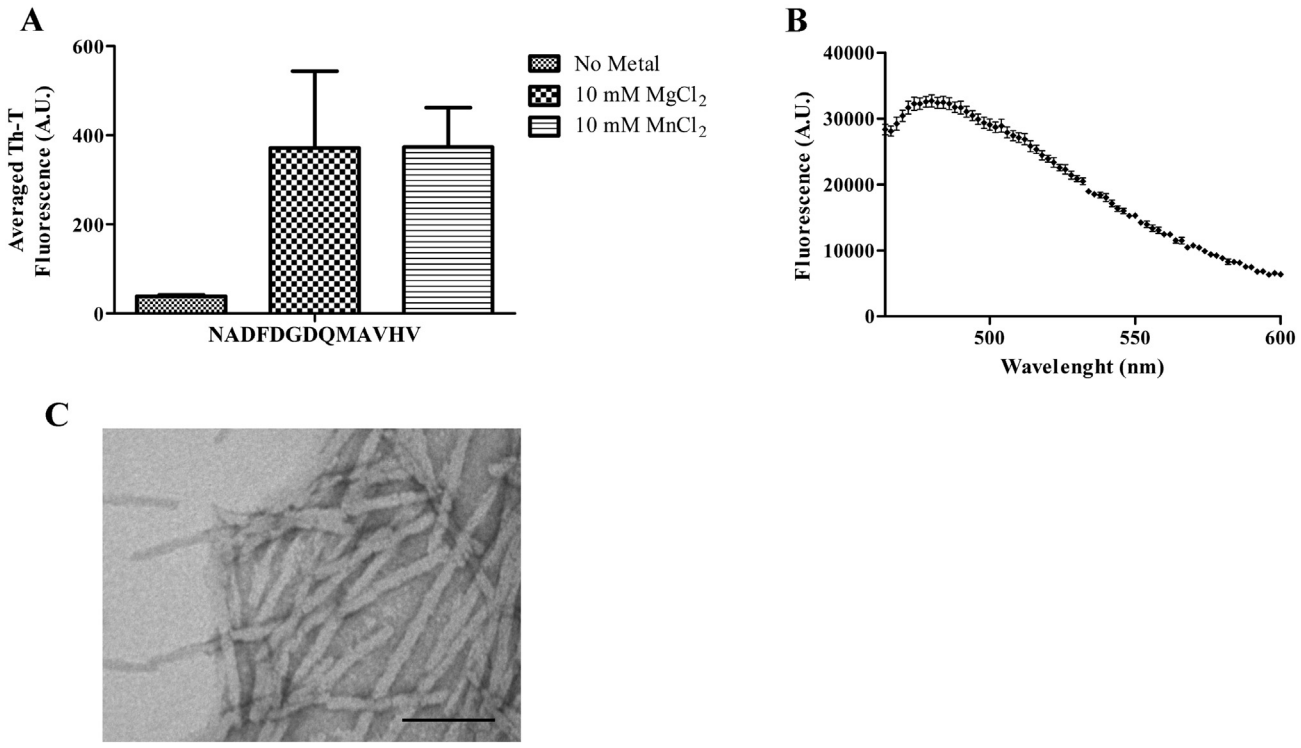


**Fig. 1. Aggregation of peptide NADFDGDQMAVHV into amyloids**. A) The Th-T emission fluorescence in arbitrary units (A.U.) measured at 480 nm was averaged from a 48-hr time-course aggregation experiment upon mixing the peptide (500 μM) with and without divalent metals at pH 8.0. B) A Th-T spectra taken from an end point in the experiment described on *A* is shown. C) TEM picture of amyloids (500 μM) grown in 10 mM $MnCl_2$ at pH 8.0 for 48 h at 37C. Scale bar is 100 nm. Errors bars represent standard error of three independent measurements.

maximum emission at around 480 nm (Fig. 1B). To further confirm the amyloid nature of the samples we analyzed the $Mn^{+2}$-induced aggregates by TEM and found the formation of typical amyloid fibrils (Fig. 1C). In order to check whether this transition was specifically induced by divalent metals without significant contribution from unspecific ionic strength effects, we incubated the peptide with the monovalent metal $K^+$ (KCl) at 50-times the concentration used with the divalent metals and found no increase in Th-T averaged signal (Fig. S1).

### 3.2. Testing the activity of the amyloid

We assayed the potential catalytic reactivity of these amyloids towards nucleotides by incubating the peptide in the same conditions as those used for aggregation and added 1 mM of a model nucleotide (ATP) as substrate. After 1 day-incubation we observed that in presence of peptide, ATP was mostly hydrolyzed to ADP and AMP compared to controls without peptides (Fig. 2A). Interestingly, this activity was observed in presence of $Mn^{+2}$ and not $Mg^{+2}$ (data not shown). We then determined the conditions to achieve initial rate ($V_0$) and measured $V_0$ at different ATP concentrations (Fig. 2B). The results show that $V_0$ follows a hyperbolic-type of dependence on substrate with apparent saturation effects starting around 0.25 mM ATP that continued until 1 mM ATP. To our surprise, ATP concentrations higher than 1 mM led to a decrease of $V_0$ that approached close-to-baseline levels at 4 mM ATP. Intrigued whether this observation was due to a possible ATP-dependent dissociation of the amyloid with a consequent decrease of the activity, we measured the amyloid formation of the peptide in presence of Th-T under the same conditions as in Fig. 2B, e.g. in presence of ATP. Interestingly, we observed no clear correlation between averaged Th-T fluorescence and ATP (Fig. 2C). Moreover, the averaged fluorescence at 4 mM ATP was very similar to that obtained at 1 mM ATP, which is the substrate concentration where the maximum observed activity was achieved.

The above results prompted us to consider that the observed substrate inhibition may be due to an active site-specific effect as it happens with enzymes that show the same phenomenon. Therefore, we adjusted the kinetic data to known models of substrate inhibition in order to obtain some enzymatic parameters. However, all curve fittings returned unreliable $K_M$ and $V_{max}$ values with very high standard errors (data not shown). We then attempted to model the data to a classic Michaelis-Menten model using ATP concentrations up to 1 mM before the contribution from substrate inhibition is significant. The obtained parameters were $V_{max} = 6.6 \pm 1.3$ μM $hr^{-1}$ and $K_M = 9.2 \pm 7.9 \times 10^{-2}$ mM (Fig. S2A). To determine a catalytic constant ($k_{cat}$) we measured $V_0$ at different peptide concentrations (Fig. S2B). The observed activity is shown to increase linearly with the peptide concentration ($R^2$ 0.93). The linear regression analysis yielded a $k_{cat} = 1.4 \pm 0.12 \times 10^{-2}$ $hr^{-1}$, leading to an estimated catalytic efficiency $k_{cat}/K_M = 2 \pm 0.13 \times 10^{-1}$ $mM^{-1}$ $hr^{-1}$.

### 3.3. Correlation between amyloid formation and activity

To determine whether the amyloid was the catalytically active species, we performed several activity experiments and analyze their association with amyloid formation. Considering that the amyloid conformation is typically reached after an aggregation lag phase, we hypothesized that the catalytic activity of the peptide will increase as the amyloids start accumulating. We therefore correlated the progress curve of the activity with the averaged Th-T signal from a time-course aggregation experiment and observed that ATP hydrolysis increased in a very similar time-dependent

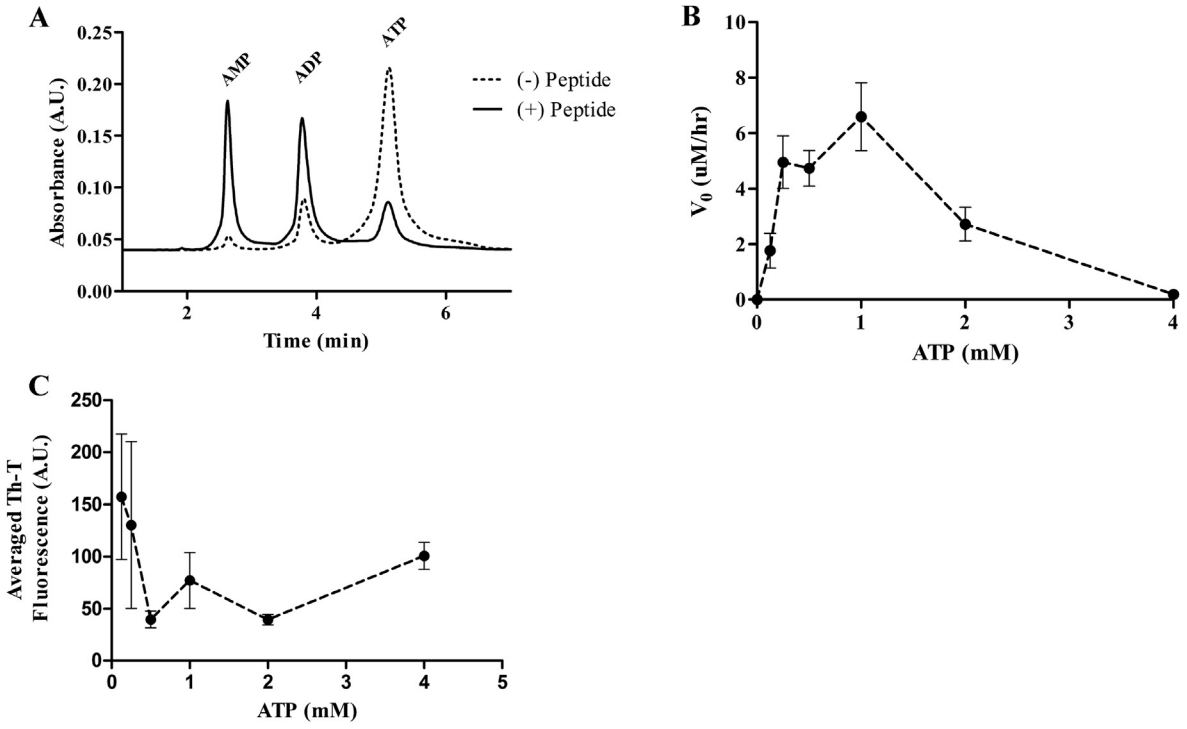


**Fig. 2. ATP hydrolysis by peptide NADFDGDQMAVHV**. A) Representative chromatogram of the reaction products (ADP and AMP) in presence or absence of peptide (500 μM) after a 24-hr reaction analyzed by HPLC. The three peaks are labeled with their corresponding nucleotides. B) Dependence of $V_0$ on ATP concentration. The hydrolytic activity from controls samples (without peptide) was subtracted from the reactions with peptide (500 μM). Data points are linearly connected to show overall profile (dotted line). C) Th-T averaged fluorescence in arbitrary units (A.U.) from time-course peptide (500 μM) aggregations at different ATP concentrations measured within $V_0$ time range (20 h). Dotted connecting line is shown to search for correlation. Errors bars represent standard error of three independent measurements.

manner as the amyloid signal (Fig. 3A). We then analyzed the dependence of the activity on the peptide concentration (shown in Fig. S2B) and correlated again the data with amyloid formation. The results show that both $V_0$ and Th-T averaged signal increase in a similar way as more peptide is added (Fig. 3B). For the final correlation experiment, we reasoned that if the amyloids are the active species, their isolation from monomers should conserve the hydrolytic activity. We therefore pre-formed the amyloids in the absence of ATP and then after centrifugation, we removed the supernatant and resuspended the aggregates using fresh buffer solution containing substrate and $Mn^{+2}$. The activity was then measured in a similar way as in Fig. 2B. We observed that the substrate concentration effect on $V_0$ obtained in this way was virtually reconstituted to what was obtained previously (Fig. 3C). From 0 to 1 mM ATP, the curve is almost indistinguishable from the data obtained without pre-formed amyloids, reaching again a maximum activity at 1 mM ATP. At 2 mM and 4 mM ATP however, the results showed higher activities with the pre-formed amyloids but still exhibited substrate inhibition.

### *3.4. Sequence-dependent analysis of activity and amyloid formation*

Since the putative catalytic aspartates are not in an amyloidogenic region, we split the original peptide in their non- amyloidogenic (NADFDGDQ) and amyloidogenic (QMAVHV) segments and determine their aggregation and activity over time. Fig. 4A shows that none of the smaller peptides was able to recapitulate the activity observed with the whole sequence. Moreover, no activity was observed with any of these peptides. We then measured the time-course aggregation of each peptide and observed that as expected, the amyloidogenic fragment exhibited around 150 times more averaged Th-T signal than the non-amyloidogenic peptide. Indeed, peptide NADFDGDQ showed a signal very close to baseline, suggesting no amyloids were formed with this peptide. The Th-T signal of the whole-sequence peptide was located in-between the signals obtained with the two smaller peptides.

## 4. Discussion

The combined data show that peptide NADFDGDQMAVHV is able to hydrolyze ATP into ADP and AMP in its amyloid conformation. The following summary of results support this idea: 1) both peptide concentration and time-dependent activity show strong correlation with time-course aggregation (if the monomer were the active species we should expect a decrease of the activity as the monomers get recruited in the amyloids); 2) aggregates separated from the soluble forms fully recapitulate the activity; 3) peptide NADFDGDQ that has the putative active sequence did not form amyloids and was inactive towards ATP. Moreover, peptide QMAVHV provides both *in silico* (Table 1) and *in vitro* (Fig. 4B) the amiloidogenicity to the whole peptide but it is also inactive. Considering this last point and the known affinity of $Mg^{+2}/Mn^{+2}$ for carboxyl groups, we can also conclude that the activity is most likely attributed to the aspartates and their specific interaction with $Mn^{+2}$.

The observed catalytic activity exhibited some canonical enzyme-like features such as substrate-dependent saturation of activity, linear activity increase with peptide concentration and substrate inhibition. Interestingly, this last feature is well known to occur in several classic enzymes with ATP-dependent activity such as Phosphofructokinase that exhibits inhibitory substrate concentrations starting around 1 mM ATP as we also observed in our data [19]. Substrate specificity was not explored in the present work or

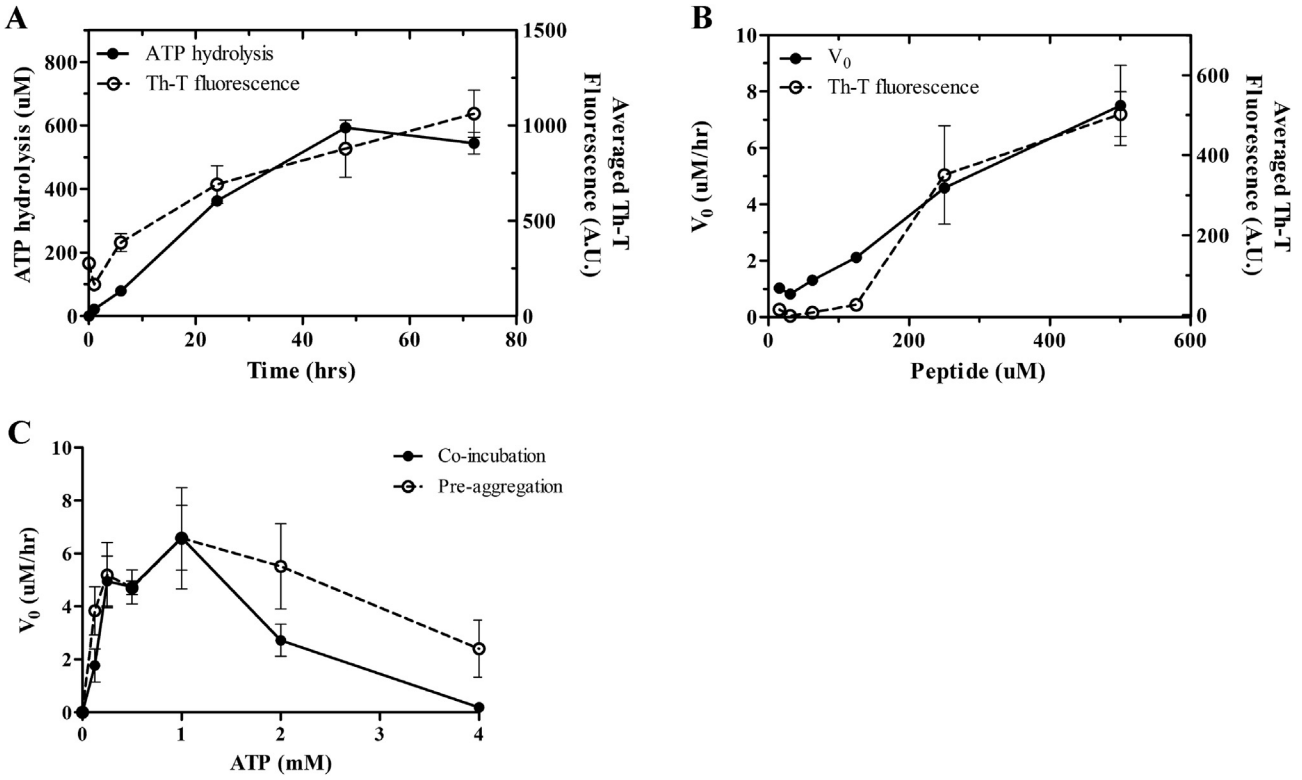


**Fig. 3. Correlation of activity with aggregation**. A) A progress curve of the activity is correlated with the time-course aggregation of the peptide (500 μM) measured as averaged Th-T fluorescence in arbitrary units (A.U.). B) Effect of peptide concentration on $V_0$ and aggregation. Amyloid formation was measured by averaging Th-T fluorescence over a 20-hr period ($V_0$ time range). Activity data is duplicated from Fig. S2B. C) Comparison of $V_0$ dependence on ATP between Co-incubation (solubilized peptide and ATP are mixed at the start of the reaction, data taken from Fig. 2B) and Pre-aggregation (amyloids are pre-formed in 10 Mm $MnCl_2$ at pH 8.0 before adding the substrate). Peptide concentration is 500 μM. Errors bars represent standard error of three independent measurements. Data points are linearly connected to show overall profiles (dotted and straight lines).

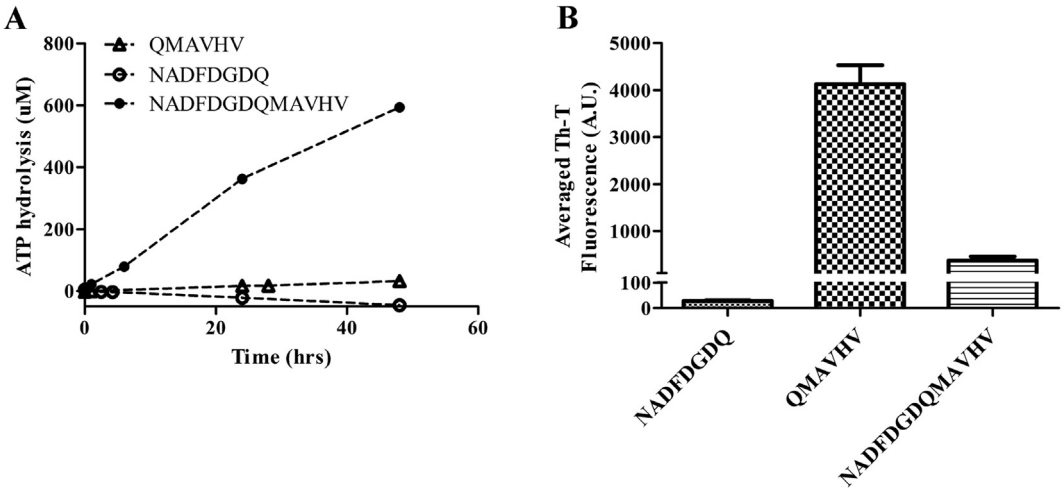


**Fig. 4. Activity and aggregation of peptide fragments from NADFDGDQMAVHV**. A) Comparison among progress curves obtained with NADFDGDQMAVHV (taken from Fig. 3A) and peptides NADFDGDQ and QMAVHV. B) Averaged Th-T fluorescence in arbitrary units (A.U.) measured from time-course aggregation experiments with peptide NADFDGDQ-MAVHV (taken from Fig. 1A) compared to peptides NADFDGDQ and QMAVHV. Errors bars represent standard error of three independent measurements. Data points are linearly connected to show overall profile (dotted line). Peptide concentration was 500 μM for both experiments.

in the previous reports on catalytic amyloids but considering the relatively simple and rigid amyloid fold it is believed that it will be limited [20].

The hydrolytic activity was observed only with $Mn^{+2}$. This metal is known to have better preference than $Mg^{+2}$ for attracting water molecules, in addition to interacting well with oxygens from all three ATP phosphates [21,22]. It is then likely that water molecules may be required for activity and thus promote hydrolysis. Consistently with this point, amyloids are known to expose their polar and charged groups to aqueous solvent keeping their hydrophobic residues buried in the amyloid core, findings that are also backed by simulations showing that water molecules can directly interact with these exposed groups [3,23,24]. All this evidence suggests that amyloid-bound $Mn^{+2}$ could have continuous and dynamic

interactions with the surrounding water. We did not observe further hydrolytic products as no additional peaks were detected by HPLC and the ATP substrate decreased in proportion to the increase in ADP and AMP products. This indicates that the amyloid is active specifically towards the phosphoanhydride bonds, suggesting an ATPase-like activity.

The rates observed in our study evidenced activities occurring within hours. Although most enzymes operate in faster regimes, their structures have typically been subjected to evolutionary constraints to achieve their known efficiencies. Moreover, ATP is known to be a kinetically very stable molecule and therefore the catalysis of its hydrolysis requires complex chemistry as it is seen in the active sites of enzymes involved in ATP hydrolysis [25]. Substrate inhibition may also have affected the observed activities by preventing the amyloid-driven hydrolysis to achieve maximum rates. In addition to that, we suspect that electrostatic repulsion between ATP and our amyloid can have a modulating effect on activity. At the reaction pH (8.0), ATP has a predominant negative charge whereas our peptide has three aspartates that should be deprotonated and thus charged, creating potentially strong repulsion. The interactions with divalent metals may partially shield this effect but without high-resolution data it is difficult to estimate this parameter. The activity of the previously reported amyloids is strictly dependent on deprotonation of the catalytic histidines to allow coordination of $Zn^{+2}$, leading to uncharged amyloids that can then react much more efficiently with the uncharged model substrate p-nitrophenylacetate at pH 8.0 [10,11].

The enzymatic-like activity parameters ($V_{max}$, $K_M$ and $k_{cat}$) were determined using a classic Michaelis-Menten model due to the difficulties encountered when fitting the data to known substrate inhibition models, however these values do not represent the real scenario. We rule out data reliability caused this situation since the observed curve (Fig. 2B) was repeated several times with similar results. Furthermore, the rates obtained with pre-formed amyloids not only reconstituted the original activity profile but also exhibited very similar $V_0$ values, indicating that the experimental data is robust (Fig. 3C). We also think that the decreasing activity at high ATP concentrations is not related to amyloid disaggregation since Th-T signal remained relatively constant (Fig. 2C). It is then possible that different mechanisms may account for the observed substrate inhibition. One scenario can imply ATP-driven conformational changes in the amyloid structure at high substrate concentrations that would lead to a somewhat inactive form. Alternatively, the yet unknown mechanistic aspects underlying catalytic reactivity in amyloids may reveal an inherent tendency towards substrate inhibition arising from potential active site heterogeneity due to the multiple binding sites along the amyloid surface. In fact, to our knowledge, this inhibitory effect at high substrate concentrations was not explored in the previous reports on catalytic amyloids and therefore its contribution cannot be ruled out from those studies. Future experiments with this and other peptides should clarify these questions.

Overall, our results show the first catalytic amyloid that is reactive towards a biologically important molecule. Large randomly-selected polypeptides (>100-residue-long) have been shown to bind ATP and exhibit modest ATP hydrolytic activity [26]. Our study demonstrates that much smaller peptides can achieve efficient activity towards the same nucleotide in a conformation that has biomedical and evolutionary relevance, paving the way for future design of even smaller and simpler peptides with for instance prebiotic amino acid composition. In addition to that, the novel finding that acidic residues can also be catalytic in the amyloid state suggests that the reactivity of these aggregates may well be a more general property with broad implications.

## Acknowledgements

This work was supported by research grant CONICYT/FONDECYT/3150054.

## Appendix A. Supplementary data

Supplementary data related to this article can be found at http://dx.doi.org/10.1016/j.bbrc.2016.12.011.

## Transparency document

Transparency document related to this article can be found online at http://dx.doi.org/10.1016/j.bbrc.2016.12.011.

## References

[1] D. Eisenberg, M. Jucker, The amyloid state of proteins in human diseases, Cell 148 (2012) 1188–1203.
[2] J. Greenwald, R. Riek, Biology of amyloid: structure, function, and regulation, Structure 18 (2010) 1244–1260.
[3] M.R. Sawaya, S. Sambashivan, R. Nelson, M.I. Ivanova, S.A. Sievers, M.I. Apostol, M.J. Thompson, M. Balbirnie, J.J. Wiltzius, H.T. McFarlane, A.O. Madsen, C. Riekel, D. Eisenberg, Atomic structures of amyloid cross-beta spines reveal varied steric zippers, Nature 447 (2007) 453–457.
[4] K.E. Marshall, R. Marchante, W.F. Xue, L.C. Serpell, The relationship between amyloid structure and cytotoxicity, Prion 8 (2014).
[5] D.M. Fowler, A.V. Koulov, W.E. Balch, J.W. Kelly, Functional amyloid–from bacteria to humans, Trends Biochem. Sci. 32 (2007) 217–224.
[6] M.R. Chapman, L.S. Robinson, J.S. Pinkner, R. Roth, J. Heuser, M. Hammar, S. Normark, S.J. Hultgren, Role of Escherichia coli curli operons in directing amyloid fiber formation, Science 295 (2002) 851–855.
[7] S.V. Paushkin, V.V. Kushnirov, V.N. Smirnov, M.D. Ter-Avanesyan, Propagation of the yeast prion-like [psi+] determinant is mediated by oligomerization of the SUP35-encoded polypeptide chain release factor, EMBO J. 15 (1996) 3127–3134.
[8] S.K. Maji, M.H. Perrin, M.R. Sawaya, S. Jessberger, K. Vadodaria, R.A. Rissman, P.S. Singru, K.P. Nilsson, R. Simon, D. Schubert, D. Eisenberg, J. Rivier, P. Sawchenko, W. Vale, R. Riek, Functional amyloids as natural storage of peptide hormones in pituitary secretory granules, Science 325 (2009) 328–332.
[9] I. Cherny, E. Gazit, Amyloids: not only pathological agents but also ordered nanomaterials, Angew. Chem. Int. Ed Engl. 47 (2008) 4062–4069.
[10] C.M. Rufo, Y.S. Moroz, O.V. Moroz, J. Stohr, T.A. Smith, X. Hu, W.F. DeGrado, I.V. Korendovych, Short peptides self-assemble to produce catalytic amyloids, Nat. Chem. 6 (2014) 303–309.
[11] M.P. Friedmann, V. Torbeev, V. Zelenay, A. Sobol, J. Greenwald, R. Riek, Towards prebiotic catalytic amyloids using high throughput screening, PLoS.One 10 (2015) e0143948.
[12] C.P. Maury, Self-propagating beta-sheet polypeptide structures as prebiotic informational molecular entities: the amyloid world, Orig. Life Evol. Biosph. 39 (2009) 141–150.
[13] J. Greenwald, M.P. Friedmann, R. Riek, Amyloid aggregates arise from amino acid condensations under prebiotic conditions, Angew. Chem. Int. Ed Engl. 55 (2016) 11609–11613.
[14] H. Naiki, K. Higuchi, M. Hosokawa, T. Takeda, Fluorometric determination of amyloid fibrils in vitro using the fluorescent dye, thioflavin T1, Anal. Biochem. 177 (1989) 244–249.
[15] M.J. Thompson, S.A. Sievers, J. Karanicolas, M.I. Ivanova, D. Baker, D. Eisenberg, The 3D profile method for identifying fibril-forming segments of proteins, Proc. Natl. Acad. Sci. U.S.A 103 (2006) 4074–4078.
[16] L. Goldschmidt, P.K. Teng, R. Riek, D. Eisenberg, Identifying the amylome, proteins capable of forming amyloid-like fibrils, Proc. Natl. Acad. Sci. U.S.A 107 (2010) 3487–3492.
[17] K. Kuchta, L. Knizewski, L.S. Wyrwicz, L. Rychlewski, K. Ginalski, Comprehensive classification of nucleotidyltransferase fold proteins: identification of novel families and their representatives in human, Nucleic Acids Res. 37 (2009) 7701–7714.
[18] L. Aravind, E.V. Koonin, DNA polymerase beta-like nucleotidyltransferase superfamily: identification of three new families, classification and evolutionary history, Nucleic Acids Res. 27 (1999) 1609–1618.
[19] R.L. Zheng, R.G. Kemp, The mechanism of ATP inhibition of wild type and mutant phosphofructo-1-kinase from Escherichia coli, J. Biol. Chem. 267 (1992) 23640–23645.
[20] T. Aumüller, M. Fändrich, Catalytic amyloid fibrils, Nat. Chem. 6 (2014) 273–274.
[21] G.C. Dismukes, Manganese enzymes with binuclear active sites, Chem. Rev. 96 (1996) 2909–2926.
[22] K. Hongo, H. Hirai, C. Uemura, S. Ono, J. Tsunemi, T. Higurashi, T. Mizobata, Y. Kawata, A novel ATP/ADP hydrolysis activity of hyperthermostable group II

chaperonin in the presence of cobalt or manganese ion, FEBS Lett. 580 (2006) 34–40.
[23] D. Thirumalai, G. Reddy, J.E. Straub, Role of water in protein aggregation and amyloid polymorphism, Acc. Chem. Res. 45 (2012) 83–92.
[24] G. Reddy, J.E. Straub, D. Thirumalai, Dry amyloid fibril assembly in a yeast prion peptide is mediated by long-lived structures containing water wires, Proc. Natl. Acad. Sci. U.S.A 107 (2010) 21459–21464.
[25] J.M. Miller, E.J. Enemark, Fundamental characteristics of AAA+ protein family structure and function, Archaea 2016 (2016) 9294307.
[26] S.K. Kang, B.X. Chen, T. Tian, X.S. Jia, X.Y. Chu, R. Liu, P.F. Dong, Q.Y. Yang, H.Y. Zhang, ATP selection in a random peptide library consisting of prebiotic amino acids, Biochem. Biophys. Res. Commun. 466 (2015) 400–405.